AIP Applied Physics Letters

Low-noise AlInAsSb avalanche photodiode

Madison E. Woodson, Min Ren, Scott J. Maddox, Yaojia Chen, Scott R. Bank, and Joe C. Campbell

Citation: Applied Physics Letters **108**, 081102 (2016); doi: 10.1063/1.4942372
View online: http://dx.doi.org/10.1063/1.4942372
View Table of Contents: http://scitation.aip.org/content/aip/journal/apl/108/8?ver=pdfcov
Published by the AIP Publishing

Articles you may be interested in
AlInAsSb/GaSb staircase avalanche photodiode
Appl. Phys. Lett. **108**, 081101 (2016); 10.1063/1.4942370

Enhanced low-noise gain from InAs avalanche photodiodes with reduced dark current and background doping
Appl. Phys. Lett. **101**, 151124 (2012); 10.1063/1.4757424

Ultralow noise midwave infrared InAs–GaSb strain layer superlattice avalanche photodiode
Appl. Phys. Lett. **91**, 241111 (2007); 10.1063/1.2817608

Monte Carlo simulation of low-noise avalanche photodiodes with heterojunctions
J. Appl. Phys. **92**, 4791 (2002); 10.1063/1.1505987

Thin multiplication region InAlAs homojunction avalanche photodiodes
Appl. Phys. Lett. **73**, 783 (1998); 10.1063/1.122000

Reuse of AIP Publishing content is subject to the terms at: https://publishing.aip.org/authors/rights-and-permissions. IP: 129.116.140.16 On: Fri, 26 Feb 2016 19:52:00

CrossMark click for updates

Low-noise AlInAsSb avalanche photodiode

Madison E. Woodson,[1] Min Ren,[1] Scott J. Maddox,[2] Yaojia Chen,[1] Scott R. Bank,[2] and Joe C. Campbell[1]
[1]*Department of Electrical and Computer Engineering, University of Virginia, Charlottesville, Virginia 22904, USA*
[2]*Microelectronics Research Center, The University of Texas, Austin, Texas 78758, USA*

(Received 9 December 2015; accepted 5 February 2016; published online 22 February 2016)

We report low-noise avalanche gain from photodiodes composed of a previously uncharacterized alloy, $Al_{0.7}In_{0.3}As_{0.3}Sb_{0.7}$, grown on GaSb. The bandgap energy and thus the cutoff wavelength are similar to silicon; however, since the bandgap of $Al_{0.7}In_{0.3}As_{0.3}Sb_{0.7}$ is direct, its absorption depth is 5 to 10 times shorter than indirect-bandgap silicon, potentially enabling significantly higher operating bandwidths. In addition, unlike other III-V avalanche photodiodes that operate in the visible or near infrared, the excess noise factor is comparable to or below that of silicon, with a k-value of approximately 0.015. Furthermore, the wide array of absorber regions compatible with GaSb substrates enable cutoff wavelengths ranging from 1 μm to 12 μm. © *2016 AIP Publishing LLC*. [http://dx.doi.org/10.1063/1.4942372]

Avalanche photodiodes (APDs) have been used for a wide range of commercial, military, and research applications. Foremost among these are optical communications,[1] imaging,[2,3] and single photon detection.[4,5] Their primary advantage relative to p-i-n photodiodes is that the APD gain can provide higher sensitivity, i.e., detection of lower signal magnitude. However, the origin of the APD gain is impact ionization, a stochastic process that results in higher shot noise. The mean-squared shot-noise current $\langle i^2_{shot}\rangle$ can be expressed as

$$\langle i^2_{shot}\rangle = 2q(I_{ph} + I_{dark})M^2F(M)\Delta f, \qquad (1)$$

where I_{ph} and I_{dark} are the primary photocurrent and dark current, respectively, M is the avalanche gain, Δf is the bandwidth, and *F(M)* is the excess noise factor. In the local field model,[6] the excess noise factor is given by $F(M) = kM + (1-k)[2 - 1/M]$, where k is the ratio of the electron, α, and hole, β, ionization coefficients such that by convention $k = \beta/\alpha$ if $\beta < \alpha$ and $k = \alpha/\beta$ if $\beta > \alpha$. The excess noise factor increases with increasing gain but increases more slowly the lower the value of k. The competition between the benefit of gain and its relationship to excess noise is illustrated by the signal to noise ratio, SNR

$$\mathrm{SNR} = \frac{\mathrm{I}^2}{2\mathrm{qIF(M)\Delta f} + \sigma^2_{\mathrm{circuit}}/\mathrm{M}^2}, \qquad (2)$$

where $\sigma^2_{\mathrm{circuit}}$ is the RMS noise current of the following amplifier. It is clear that until the gain becomes high enough for the excess noise to dominate the total noise, the APD gain effectively suppresses the amplifier noise. Thus, low excess noise, i.e., low k-values, are highly desirable. It should be noted that low k values also yield high gain-bandwidth products.[7]

The most straight-forward method of achieving low noise is to select a semiconductor with favorable ionization coefficients; for this reason, Si, which exhibits a low k-value of ~0.04, is the material of choice for APDs that operate in the visible and near-infrared (<900 nm). The absorption length, d, which defined as the thickness required to achieve ~90% internal quantum efficiency, can be expressed as $d \approx 2/\alpha$, where α is the absorption coefficient. Since Si is an indirect semiconductor, its absorption length increases from approximately 5 μm at 600 nm to >15 μm at 900 nm.[8,9] The long absorption length results in long transit time and concomitant low bandwidth. While higher bandwidths are readily achieved with direct bandgap semiconductors such as GaAs and InP, their excess noise factors are characterized by high k values, ~0.5. Recently, we have demonstrated growth of high-quality $Al_xIn_{1-x}As_ySb_{1-y}$ digital alloys lattice-matched to GaSb, for use in staircase APDs.[10] Previous lattice-matched growths of the material have achieved only as much as a 30% aluminum fraction,[11,12] although there has been success growing material with up to 60% aluminum fraction without lattice matching.[13] We have achieved 70% aluminum fractions as high as 80% by inserting an additional AlAs layer into each digital alloy period, maintaining lattice-matching and thus low dark current. Moreover, direct bandgap materials, such as $Al_{0.7}In_{0.3}As_{0.3}Sb_{0.7}$, typically exhibit absorption lengths ~2 μm and, thus, higher bandwidths than their Si counterparts. In this paper, we report the study of a p-i-n structure APD fabricated from this material. These APDs offer the advantages of III-V compound direct bandgap APDs with regard to high absorption coefficient and a lattice-matched material system that provides the flexibility to design complex structures to maximize performance and enable operation in different spectral regions.[10] In addition, these direct-bandgap APDs exhibit bulk excess noise comparable to Si without taking advantage of the dead-space effect in a thin multiplication region.[14–17]

The samples in this study were grown on n-type Te-doped GaSb (001) substrates by solid-source molecular beam epitaxy (MBE). In order to bypass the wide miscibility gap present in the $Al_xIn_{1-x}As_ySb_{1-y}$ material system, these layers were grown as a digital alloy of the binary alloys AlAs, AlSb, InAs, and InSb, using a digital alloy period of 3 nm and the following shutter sequence: AlSb, AlAs, AlSb, InSb, InAs, Sb. Further details of the growth and properties

 © 2016 AIP Publishing LLC

Reuse of AIP Publishing content is subject to the terms at: https://publishing.aip.org/authors/rights-and-permissions. IP: 129.116.140.16 On: Fri, 26 Feb 2016 19:52:00

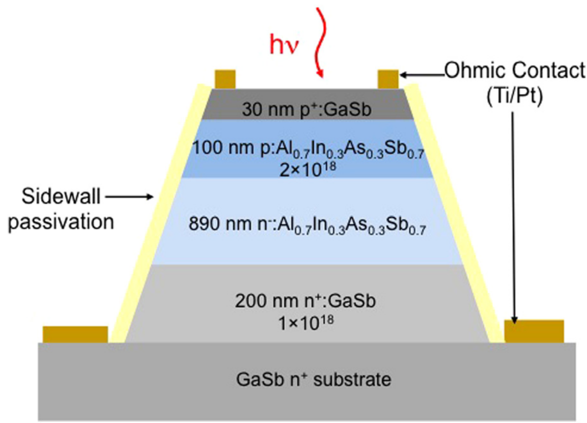

FIG. 1. Cross-sectional schematic of $Al_{0.7}In_{0.3}As_{0.3}Sb_{0.7}$ avalanche photodiode.

of the resulting $Al_xIn_{1-x}As_ySb_{1-y}$ digital alloy films are provided elsewhere.[18–20]

A cross-sectional schematic of the $Al_{0.7}In_{0.3}As_{0.3}Sb_{0.7}$ device is shown in Fig. 1. The structure includes a top GaSb layer to reduce contact resistance, improve contact adhesion, and protect the underlying Al-containing layers from oxidation. Circular mesas were defined using standard photolithography and wet-etched using an $HCl:H_2O_2:H_2O$ solution. Etching was terminated with a surface-smoothing treatment of bromine methanol. In order to improve passivation and thus reduce the surface leakage current, an SU-8 coating was spun on immediately after the surface treatment. Titanium/gold contacts were deposited by e-beam evaporation onto the mesa and the substrate. For some devices, the GaSb top contact layer was removed except under the p-type contacts, in order to eliminate its parasitic optical absorption. AZ 300 was used to selectively etch the GaSb prior to SU-8 coating.

All measurements in this paper were carried out at room temperature. Figure 2 shows the dark current, photocurrent, and gain versus voltage for a 30 μm-diameter $Al_{0.7}In_{0.3}As_{0.3}Sb_{0.7}$ APD. The slight increase in photocurrent at low bias reflects the increase in depletion width in the n^- layer. Capacitance-voltage measurements are shown in Fig. 3, indicating that this layer is fully depleted at -3 V. From -3 V to -25 V, the photocurrent is relatively independent of the bias voltage. The photocurrent at -5 V bias was designated as the unity gain point of the device. Breakdown occurred at a reverse bias of 40.5 V, corresponding to a peak electric field of ~530 kV/cm. The maximum stable gain reached before breakdown was 95. The dark current was ~4 nA (6×10^{-4} A/cm^2) at 90% of breakdown. Total leakage current, I_D, can be expressed as: $I_D = I_{DS} + I_{DB}M$, where I_{DB} *is* the multiplied dark current and I_{DS} is the surface leakage current. Figure 4 shows the dark current versus gain for a 30 μm-diameter $Al_{0.7}In_{0.3}As_{0.3}Sb_{0.7}$ APD. The linear fit corresponds to $I_{DS} \approx 6$ nA and $I_{DB} \approx 0.14$ nA. These measurements indicate that leakage is surface dominated, but further study of passivation techniques promise to push toward bulk leakage, further decreasing dark current values.

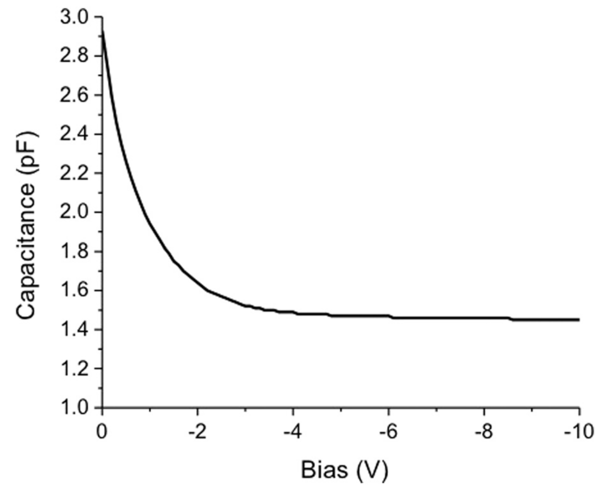

FIG. 3. Capacitance versus bias for a 100 μm-diameter $Al_{0.7}In_{0.3}As_{0.3}Sb_{0.7}$ avalanche photodiode.

Figure 5 shows the external quantum efficiency versus wavelength at -5 V bias. Measurements were taken using a tungsten-halogen light source, a monochrometer, and a lock-in amplifier. The measured data were referenced to a calibrated silicon photodiode. Collection of electrons created by absorption in the GaSb top contact layer is poor due to surface recombination and a barrier at the $GaSb/Al_{0.7}In_{0.3}As_{0.3}Sb_{0.7}$

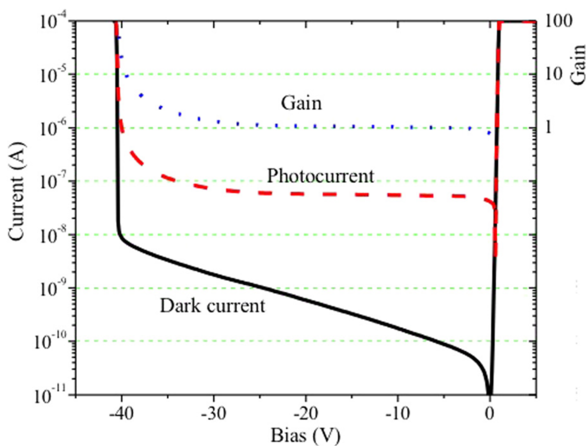

FIG. 2. Dark current (solid line), photocurrent (dashed line), and gain (dotted line) versus bias for a 30 μm-diameter $Al_{0.7}In_{0.3}As_{0.3}Sb_{0.7}$ avalanche photodiode.

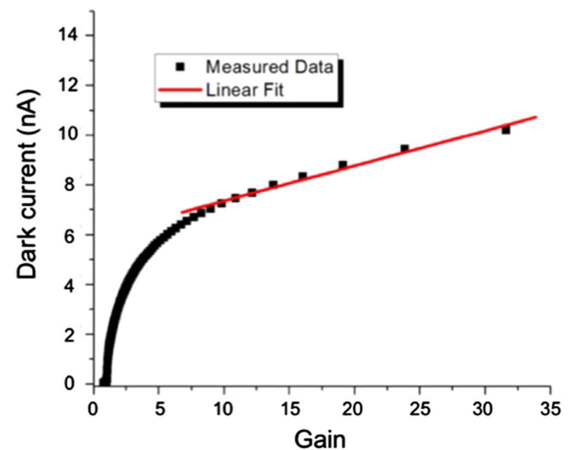

FIG. 4. Dark current characteristics of 30 μm-diameter $Al_{0.7}In_{0.3}As_{0.3}Sb_{0.7}$ avalanche photodiode. The linear fit shows that the primary multiplied dark current is 6 nA and the unmultiplied dark current, which is typically associated with surface leakage is 0.14 nA.

Reuse of AIP Publishing content is subject to the terms at: https://publishing.aip.org/authors/rights-and-permissions. IP: 129.116.140.16 On: Fri, 26 Feb 2016 19:52:00

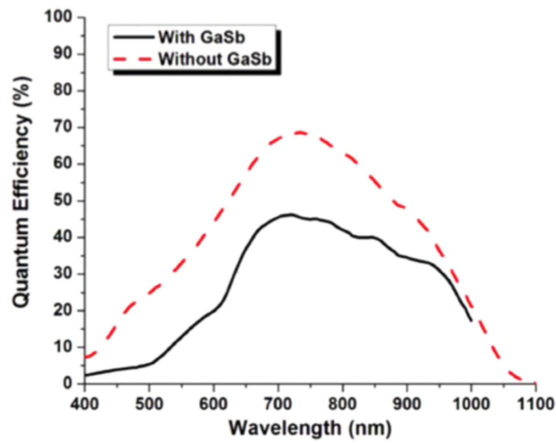

FIG. 5. External quantum efficiency versus wavelength for devices with and without the top GaSb layer.

interface. Prior to removing the GaSb layer, the quantum efficiency is above 30% for wavelengths between 630 nm and 960 nm, peaking at 46% at 715 nm. After its removal, the efficiency increases as much as 20% from 500 nm to 850 nm, reaching ~68% near 700 nm. We note that an anti-reflection coating has not been applied to these devices. If the absorption coefficient, which is not yet known for this material system, is on the order of $10^4\,\mathrm{cm}^{-1}$, since the air-semiconductor reflectivity without and antireflection coating is ~30%, a maximum efficiency of ~70% would be expected, which is close to the measured value. The long-wavelength cutoff is near 1.1 μm, which is the same as that of Si. However, by reducing the Al content in the $Al_xIn_{1-x}As_ySb_{1-y}$ to 60% the cutoff can be pushed to ~1.2 μm, which will cover the 1.064 μm wavelength of Nd:YAG lasers.

Figure 6 shows the excess noise figure, as a function of the multiplication gain, for both an $Al_{0.7}In_{0.3}As_{0.3}Sb_{0.7}$ APD (■) and a Si APD (▲) measured by an HP 8970 noise figure meter. The solid lines are plots of the excess noise for k-values from 0 to 0.6 using the local-field model.[6] The measured $Al_{0.7}In_{0.3}As_{0.3}Sb_{0.7}$ APD excess noise corresponds to an estimated k-value of 0.015 for the unity gain point at -5 V bias and does not exceed 0.05 if the unity gain point is selected up to -25 V, beyond which it is clear that there is sufficient impact ionization as to create gain. This k-value is comparable to the Si APD. For several decades, Si APDs have been the standard for low noise and InP is the material most widely deployed for telecommunications APDs. The k values for commercial Si APDs fall between 0.02 and 0.06, while InP typically exhibits k values between 0.45 and 0.52, as denoted by the shaded region in Fig. 6. We note that these k values are those of bulk material and that for high electric fields, as commonly found in the multiplication regions of separate multiplication and absorption APDs, the k values can be higher. Given the relatively thick multiplication regions of the APDs reported here, we suggest that the measured k values reflect the bulk ionization characteristics of $Al_{0.7}In_{0.3}As_{0.3}Sb_{0.7}$. Low k factor values have been observed for detectors fabricated from its constituent materials InAs[21,22] and InSb.[23] Those materials are characterized by very low electron masses, large hole masses, and large separation between the Γ conduction band minimum and the X and L satellite valleys. The scattering rates for impact ionization tend to be higher than phonon scattering to the satellite valleys. Additionally, previous studies have shown that the addition of Al to a material does not significantly increase its k-value, as with AlAsSb[24] and InAlAs.[25] Furthermore, initial Monte Carlo studies indicate that a high hole scattering rate may contribute further to the low k-value.

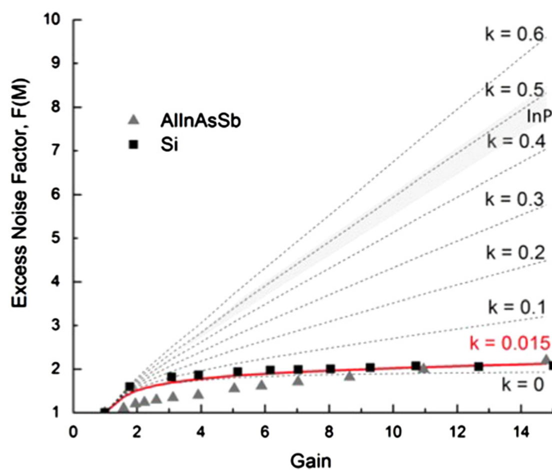

FIG. 6. Measured excess noise factor versus gain for an $Al_{0.7}In_{0.3}As_{0.3}Sb_{0.7}$ APD (■) and a Si APD (▲). The solid lines are plots of the excess noise factor using the local field model for k values from 0 to 0.5. Both the Si and $Al_{0.7}In_{0.3}As_{0.3}Sb_{0.7}$ APD are characterized by a k value of 0.015. The shaded region for $k \geq 0.45$ denotes typical values for APDs that employ InP multiplication regions.

In the expression for the shot noise of an APD, Eq. (1), the excess noise factor is multiplied by the square of the gain. It follows that small changes in the excess noise factor can result in significantly higher noise. In addition to low noise, lower k values are linked to high gain-bandwidth product. The gain-bandwidth product results from the time required for the avalanche process to build up and decay; the higher the gain, the higher the associated time constant and, thus, the lower the bandwidth. Emmons has shown that the frequency-dependent gain can be approximated by the expression[7]

$$M(f) = \frac{M_0}{\sqrt{1 + (2\pi f M_0 k \tau)^2}}, \tag{3}$$

where M_0 is the dc gain and τ is approximately (within a factor of ~2) the carrier transit time across the multiplication region. It follows from this expression that for $M_0 > 1/k$ the frequency response is characterized by a constant gain bandwidth-product that increases as k decreases. Given the measured k values of the $Al_{0.7}In_{0.3}As_{0.3}Sb_{0.7}$ APDs reported in this work, gain-bandwidth products comparable to those of Si, which have been reported to be as high as 340 GHz,[26] are anticipated.

We report an avalanche photodiode, fabricated from $Al_{0.7}In_{0.3}As_{0.3}Sb_{0.7}$, with low excess noise corresponding to $k = 0.015$ and peak quantum efficiency of 68% at 735 nm. Furthermore, since $Al_{0.7}In_{0.3}As_{0.3}Sb_{0.7}$ has a direct bandgap, it has the potential for higher bandwidths than Si, which is typically limited by transit times. The materials system promises an innovative alternative to Si for detection across the visible and near-infrared wavelengths.

Reuse of AIP Publishing content is subject to the terms at: https://publishing.aip.org/authors/rights-and-permissions. IP: 129.116.140.16 On: Fri, 26 Feb 2016 19:52:00

[1]J. C. Campbell, "Advances in photodetectors," in *Optical Fiber Telecommunications, Vol. 5, Part A: Components and Subsystems*, 5th ed., edited by I. Kaminow, T. Li, and A. E. Wilner (Academic Press, 2008).
[2]N. Bertone and W. R. Clark, Laser Focus World **43**, 69 (2007).
[3]P. Mitra, J. D. Beck, M. R. Skokan, J. E. Robinson, J. Antoszewski, K. J. Winchester, A. J. Keating, T. Nguyen, K. K. M. Silva, C. A. Musca, J. M. Dell, and L. Farone, Proc. SPIE **6232**, 62320G (2006).
[4]A. Tosi, N. Calandri, M. Sanzaro, and F. Acerbi, IEEE J. Sel. Top. Quantum Electron. **20**, 3803406 (2014).
[5]X. Jiang, M. Itzler, K. O'Donnell, M. Entwistle, M. Owens, K. Slomkowski, and S. Rangwala, IEEE J. Sel. Top. Quantum Electron. **21**, 3800112 (2015).
[6]R. J. McIntyre, IEEE Trans. Electron Devices **ED-13**, 164 (1966).
[7]R. B. Emmons, J. Appl. Phys. **38**, 3705 (1967).
[8]G. G. Macfarlane, T. P. McLean, J. E. Quarrington, and V. Roberts, Phys. Rev. **111**, 1245 (1958).
[9]E. O. Kane, J. Phys. Chem. Solids **1**, 82 (1956).
[10]S. J. Maddox, S. D. March, and S. R. Bank, "Broadly Tunable AlInAsSb Digital Alloys Grown on GaSb," J. Cryst. Growth Design (submitted).
[11]A. N. Semenov, V. A. Solov'ev, B. Y. Meltser, Y. V. Terent'ev, L. G. Prokopova, and S. V. Ivanov, J. Cryst. Growth **278**, 203 (2005).
[12]W. L. Sarney, S. P. Svensson, D. Wang, D. Donetsky, G. Kipshidze, L. Shterengas, Y. Lin, and G. Belenky, J. Cryst. Growth **425**, 357 (2015).
[13]G. Belenky, D. Wang, Y. Lin, D. Donetsky, G. Kipshidze, L. Shterengas, D. Westerfeld, W. L. Sarney, and S. P. Svensson, Appl. Phys. Lett. **102**, 111108 (2013).
[14]Y. Okuto and C. R. Crowell, Phys. Rev. B **10**, 4284 (1974).
[15]M. M. Hayat, B. E. A. Saleh, and M. C. Teich, IEEE Trans. Electron Devices **39**, 546 (1992).
[16]K. F. Li, S. A. Plimmer, J. P. R. David, R. C. Tozer, G. J. Rees, P. N. Robson, C. C. Button, and J. C. Clark, IEEE Photonics Technol. Lett. **11**, 364 (1999).
[17]J. C. Campbell, S. Chandrasekhar, W. T. Tsang, G. J. Qua, and B. C. Johnson, J. Lightwave Technol. **7**, 473 (1989).
[18]L. G. Vaughn, "Mid-infrared multiple quantum well lasers using digitally grown aluminum indium arsenic antimonide barriers and strained indium arsenic antimonide wells," Ph.D. dissertation (The University of New Mexico, New Mexico, 2006).
[19]L. G. Vaughn, L. R. Dawson, E. A. Pease, L. F. Lester, H. Xu, Y. Jiang, and A. L. Gray, Proc. SPIE **5722**, 307–318 (2005).
[20]L. G. Vaughn, L. Dawson, Ralph, H. Xu, Y. Jiang, and L. F. Lester, in Characterization of AlInAsSb and AlGaInAsSb MBE-grown digital alloys (Mat. Res. Soc. Symp. Proc., 2003), Vol. 744, pp. M7.2.1–M7.2.12.
[21]A. R. J. Marshall, C. H. Tan, M. J. Steer, and J. P. R. David, IEEE Photonics Technol. Lett. **21**, 866 (2009).
[22]S. J. Maddox, W. Sun, Z. Lu, H. P. Nair, J. C. Campbell, and S. R. Bank, Appl. Phys. Lett. **101**, 151124 (2012).
[23]R. D. Baertsch, J. Appl. Phys. **38**, 4267 (1967).
[24]C. H. Tan, S. Xie, and J. Xie, IEEE J. Quantum Electron. **48**, 36 (2011).
[25]C. Lenox, P. Yuan, H. Nie, O. Baklenov, C. Hansing, J. C. Campbell, A. L. Holmes, Jr., and B. G. Streetman, Appl. Phys. Lett. **73**, 783 (1998).
[26]Y. Kang, H.-D. Liu, M. Morse, M. J. Paniccia, M. Zadka, S. Litski, G. Sarid, A. Pauchard, Y.-H. Kuo, H.-W. Chen, W. S. Zaoui, J. E. Bowers, A. Beling, D. C. McIntosh, X. Zheng, and J. C. Campbell, Nat. Photonics **3**, 59 (2009).

Reuse of AIP Publishing content is subject to the terms at: https://publishing.aip.org/authors/rights-and-permissions. IP: 129.116.140.16 On: Fri, 26 Feb 2016 19:52:00